Contact Charge Electrophoresis: Fundamentals and Microfluidic Applications

Kyle J. M. Bishop,[*,†] Aaron M. Drews,[‡] Charles A. Cartier,[¶] Shashank Pandey,[†] and Yong Dou[†]

†*Department of Chemical Engineering, Columbia University, New York, NY*

‡*Department of Nanoengineering, University of California, San Diego, CA*

¶*Department of Chemical Engineering, Pennsylvania State University, State College, PA*

E-mail: kyle.bishop@columbia.edu

Abstract

Contact charge electrophoresis (CCEP) uses steady electric fields to drive the oscillatory motion of conductive particles and droplets between two or more electrodes. In contrast to traditional forms of electrophoresis and dielectrophoresis, CCEP allows for rapid and sustained particle motions driven by low-power DC voltages. These attributes make CCEP a promising mechanism for powering active components for mobile microfluidic technologies. This Feature Article describes our current understanding of CCEP as well as recent strategies to harness it for applications in microfluidics and beyond.

Introduction

In 1745, the Scotch Benedictine monk Andrew Gordon suspended a small metal sphere by a fine silk thread between two electrified bells.[1] He marveled as the sphere oscillated steadily between the bells, creating a gentle ringing sound (Fig. 1a). Years later, Benjamin Franklin combined Gordon's chimes with his recent invention, the lightning rod, to provide audible warning of approaching thunderstorms to further his own investigations of atmospheric electricity.[2] Franklin later noted the remarkably small amount of charge needed to drive the oscillator, and reported nearly indefinite operation of the chimes if the air were removed by means of an evacuated chamber. Legend has it that he left the bells audibly ringing during a trip to Europe, to his wife's great irritation.[1]

These early investigations of Gordon's chimes mark the first application of electricity to perform mechanical work – that is, the first electric motors. Franklin took this new idea further with his "electric wheel", which used the repeated charging and electrostatic actuation of brass thimbles mounted on a carousel to drive steady rotational motions (Fig. 1b).[3] In a world of powerful steam engines and water wheels, the electrostatic motor was merely a curiosity – Franklin himself suggested its use in an autonomous turkey rotisserie. In 1821, Michael Faraday demonstrated a superior electric motor based on electromagnetic forces, which continue to power our electric appliances and vehicles today. By contrast, the electrostatic motor faded into the annals of history, revived only for the occasional science demonstration.[6]

Now this ca. 250 year-old technology has found new life in powering particle motions and mechanical functions at the micro- and nanoscales. In a process called contact charge electrophoresis (CCEP), a conductive particle[4,5,7–11] (or droplet[12–19]) is first charged by contact with an electrode surface in the presence of an electric field and then actuated by that field via electrophoresis. Each time the particle contacts an electrode, its charge changes sign and its velocity changes direction (Fig. 1c). CCEP offers several unique characteristics that distinguish it from related forms of electric actuation such as electrophoresis (EP) and dielec-

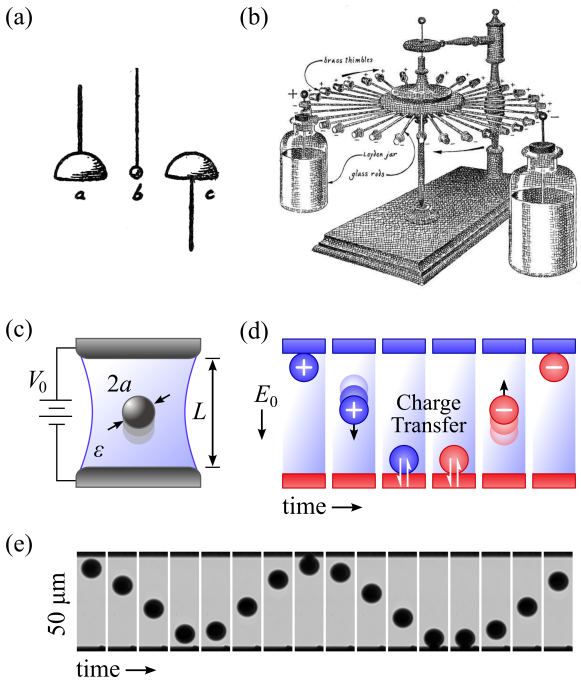

Figure 1: (a) Gordon's chimes as described in 1752.[1] (*image is public domain*) A small metal clapper b was positioned between two metal bells (a and c). An electrostatic voltage between the bells caused the clapper to oscillate continuously. (b) Franklin's electric wheel.[3] (*image is public domain*) (c) Experimental schematic of a conductive particle immersed in a dielectric fluid between two electrodes. (Adapted from reference 4 with permission of The Royal Society of Chemistry.) (d) Basic mechanism of contact charge electrophoresis. (Adapted from reference 4 with permission of The Royal Society of Chemistry.) (e) Optical images of a 10 µm silver-coated glass particle subject to a constant electric field ($E_0 = 2.5$ V µm^{-1}) at intervals of 24 ms. The particle oscillates indefinitely between the electrodes as long as the voltage is applied. (Reproduced from reference 5; copyright 2015 American Chemical Society.)

trophoresis (DEP). Most notably, CCEP allows for rapid, sustained particle motion driven by constant voltages with small energy inputs. These attributes make CCEP an attractive mechanism for powering the active components needed for mobile (i.e., small, battery powered) microfluidic technologies such as those used in Point-of-Care diagnostics.[20,21] To capitalize on these advantages, one must look beyond simple oscillatory motions and develop strategies for rectifying CCEP dynamics to perform useful functions.

This Feature Article presents our perspective on the coming renaissance of electrostatic motors in microfluidics and active colloidal systems. We introduce the basic characteristics of

CCEP, highlighting the key distinctions between this mechanism and more common forms of electric particle actuation such as EP and DEP. We review the fundamental physics underlying contact charging and particle dynamics, emphasizing open questions on the role of particle shape and on the collective behaviors of many-particle systems. We describe recent applications of CCEP motions in powering microfluidic unit operations such as particle transport, separations, and fluid mixing. Looking forward, we discuss two frontiers in the study and application of CCEP: the realization of electrostatic motors and machines at the nanoscale and the creation of active macroscopic materials based on coupled electrostatic oscillators. Ultimately, it is our hope that the long-neglected phenomenon of CCEP will find its place along side other widely used methods for electric particle manipulation.

Basic Characteristics of CCEP

The simplest realization of CCEP is illustrated in Figure 1e, which shows the rapid oscillatory motion of a conductive sphere (radius, $a = 5$ µm) immersed in mineral oil between two electrodes subject to a constant voltage. The particle acts as a mechanical "shuttle" that transports charge between the two electrodes.[8,9] When it makes electrical contact with the electrode surface, the particle acquires a net charge such that its voltage is equal to that of the electrode. Now charged, the particle migrates under the influence of the electric field with a velocity determined by the balance of the electrostatic force and the hydrodynamic drag force. Each time the particle contacts an electrode its charge changes sign, and its velocity changes direction.

This basic mechanism – combining contact charging and electrostatic actuation – is no different than that of Gordon's chimes discovered more than two centuries ago. More recently, the motion of conductive particles in dielectric liquids subject to strong electric fields has been studied to understand how the presence of such particles affects the conductivity and dielectric strength of insulating liquids.[7,8,22] Electromechanical "charge shuttles", as they

are sometimes called, have also been studied for their potential relevance to micro- and nano-electromechanical systems.[23,24] In addition to solid particles, liquid droplets have been shown to "bounce" off electrodes[12,13,16,25–27] or even liquid interfaces[14,28] by an analogous mechanism. The electrophoresis of charged drops (ECD[16]) in dielectric fluids enables new strategies for manipulating aqueous droplets within microfluidic systems.[29,30] Here, we focus our discussion on the motions of *solid* particles moving in *viscous* fluids, in which the effects of fluid and particle inertia can be neglected.

Scaling Analysis

CCEP dynamics are governed primarily by two processes: contact charging, the acquisition of charge by a conductive particle upon contact with an electrode, and electrophoresis, the movement of the now-charged particle in the applied electric field. The following order-of-magnitude analysis of these processes shows how CCEP motions depend on system parameters such as the particle radius a, the electrode separation L, and the electric field strength $E_0 = V_0/L$; a more rigorous analysis is provided below. To estimate the charge acquired by the sphere, consider that the charge density on the electrode surface is εE_0 where ε is the permittivity of the liquid. When the sphere makes electrical contact with the electrode, the charge induced on its surface can be approximated as the charge density times the surface area, $q \sim 4\pi a^2 \varepsilon E_0$. The charged particle experiences an electric force in the field as approximated by that on a point charge, $F_E \sim qE_0$. At low Reynolds numbers, the resulting motion of the particle through its viscous surroundings creates a drag force that can be approximated by Stokes law $F_H \sim 6\pi a\eta U$, where η is the fluid visocity. At steady-state, the particle velocity U is determined by equating the electrostatic and hydrodynamic forces to obtain $U \sim \varepsilon a E_0^2/\eta$. This approximate relation has been confirmed by several experimental studies[5,7–9,31] and helps to illustrate the key characteristics of CCEP motion.

Carrier Liquid

CCEP is only effective in dielectric fluids with sufficiently low electrical conductivity (e.g., mineral oil,[10] toluene,[8] silicone oil[32]). A charged particle immersed in a fluid of conductivity K will discharge on a time scale, $\tau_d \sim \varepsilon/K$. To sustain continuous motion, this charge relaxation time must be slow relative to the time between contact charging "collisions" (typically, ∼1 ms). Consequently, CCEP is effective in mineral oil ($\tau_d \sim 10$ s) but ineffective in deionized water ($\tau_d \sim 10$ µs).[10] By contrast, traditional electrophoresis is effective in high dielectric solvents (typically, water), in which ions are soluble and particles can acquire a significant surface charge (e.g., by dissociation of ionizable surface groups). In low dielectric (nonpolar) solvents, the spontaneous charging of particle surfaces requires additives such as surfactants that stabilize dissociated ions and increase the electrical conductivity of the liquid;[33–35] without such additives, electrophoresis becomes ineffective and/or unreliable. CCEP therefore offers an attractive alternative to traditional EP for the electric manipulation of particles in organic or organofluorine solvents – common carrier fluids for droplet-based microfluidics.

Particle Material

CCEP can be used to manipulate electrically conductive particles that can charge and discharge upon contact with the electrodes (or other particles). Examples include metallic or metal-coated colloids, aqueous droplets,[12–19] hydrogel particles,[4] and even suspensions of living cells.[32] CCEP of dielectric particles is also possible;[11] however, particle charging occurs much more slowly through a different mechanism (presumably contact electrification[36,36]). We limit our discussion to conductive particles in insulating fluids, for which CCEP time scales are much longer than the charge relaxation time of the particle but much shorter than that of the fluid.

Electrodes

The electrodes can be fabricated from any conductive material including metals, hydrogel electrolytes, or even aqueous solutions.[14] In contrast to EP and DEP, CCEP requires direct (electrical) contact between the particle and the electrode surface to allow for particle charging / discharging. Once charged, however, a particle can be manipulated "remotely" via traditional EP. Notably, the surface charge acquired by contact charging is much larger than that acquired spontaneously, resulting in large electrophoretic mobilities. The characteristic surface potential due to the applied field, aE_0, is often three orders of magnitude larger than the thermal potential, k_BT/e. Phenomena due to thermal motions such as the diffuse double layer and the particle zeta potential are invariably neglected.

Continuous Motion

Most importantly, CCEP allows for continuous particle motion using constant voltages; the particle shown in Figure 1e will "bounce" indefinitely as long as the voltage is maintained. In this sense, CCEP is similar to a DC electric motor, which converts electrical energy into sustained motion. By contrast, DEP of a polarizable particle in an electric field gradient relaxes to a steady equilibrium state: the particle moves to the region of highest (or lowest) field strength and stops. Similarly, in electrophoresis, a charged particle moves from one electrode to the other and stops. As discussed below, the ability to achieve continuous motion using CCEP can lead to rapid particle transport, whereby strong electrostatic forces drive steady motions perpendicular to the field over long distances.

Low Power Operation

CCEP converts electrical energy into mechanical motion with high efficiency to enable rapid particle motions at low input power. The electric current through the circuit is due almost entirely to the motion of the charged particle. For a single particle, the average current

scales as $I \sim qU/L$ and the input power as $P \sim IV_0$, which is of order 10 nW for a 30 µm sphere oscillating at 500 Hz.[5] Little or no energy is wasted in the absence of particle motion. By contrast, EP requires large faradaic currents to maintain steady electric fields within conductive liquids; these currents lead to significant dissipative losses even in the absence of particle motion.[37] The low power requirements of CCEP is attractive for use in portable microfluidic systems.

Scalability

Like other forms of electrostatic actuation, CCEP is highly amenable to miniaturization. For a constant applied voltage, the electrostatic force depends the ratio between the particle size and the electrode separation, $F_E \propto (a/L)^2$. By holding this ratio constant, the size of the system can be reduced without altering the magnitude of the electric force driving particle motion. By contrast, viscous drag and short-ranged surface forces (e.g., van der Waals) scale linearly with size;[38] they decrease in magnitude as the system is miniaturized. As a result, the particle velocity actually increases as the size of the system is decreased – that is, $U \propto a^{-1}$ for constant a/L and V_0. For example, we've observed that the particle velocity increases from $\sim$7 mm s^{-1} to more than 100 mm s^{-1} as its diameter is reduced from 13 µm to 1.5 µm. These scaling laws highlight the potential of CCEP for actuation at the micro- and nanoscales.

Fundamentals of CCEP

The charging of a conductive particle on contact with a biased electrode and its subsequent motion in the field are well described by a combination of classical electrostatics[39,40] and low Reynolds number hydrodynamics.[41,42] In this section, we discuss the physics underlying the processes of contact charging and particle motion. In addition to the well-studied case of a single sphere moving between parallel electrodes,[5] we highlight recent work on the study of

asymmetric particles and of many interacting particles.

Contact Charging

Thermodynamics of Charging

When a conductive particle makes electrical contact with an electrode surface, charge flows to/from the particle until electric equilibrium is achieved. At equilibrium, the electric potential difference between the particle and the electrode is equal to the contact potential difference characteristic of the two materials. This finite potential difference is often neglected due to the comparatively large voltages applied in CCEP experiments (typically, $10^2 - 10^4$ V). The charge acquired by the particle can be estimated by first solving the Laplace equation for the electric potential ϕ within the dielectric fluid

$$\nabla^2 \phi = 0, \tag{1}$$

subject to the follow conditions at the surfaces of the respective conductors

$$\phi(\boldsymbol{x}) = 0 \text{ for } \boldsymbol{x} \in \text{particle, electrode 1}, \tag{2}$$

$$\phi(\boldsymbol{x}) = V_0 \text{ for } \boldsymbol{x} \in \text{electrode 2}. \tag{3}$$

The net charge on the particle is then obtained by integrating the surface charge density over the particle surface

$$q = \int_{S_p} -\varepsilon \boldsymbol{n} \cdot \nabla \phi dS, \tag{4}$$

where $\boldsymbol{n}$ is the unit normal vector directed out from the particle surface. For a conductive sphere in contact with a plane electrode and subject to an applied field E_0, the charge can be computed analytically to obtain[43–46]

$$q_m = \frac{2}{3}\pi^3 \varepsilon a^2 E_0. \tag{5}$$

We refer to this result as the *Maxwell charge* as it was first obtained by Maxwell for the closely related problem of two contacting spheres.[43] The presence of a second co-planar electrode separated by a distance L results in an additional contribution of order $(a/L)^3$, which is typically neglected when $L \gg a$.[47]

The Maxwell charge of equation (5) is often considered as the "ideal" charge expected for a particle undergoing CCEP, and its accuracy has been evaluated for a variety of systems. Experimental measurements on solid conductive spheres generally agree with the theory;[7–9,31,48,49] however, systematic deviations have been observed under certain conditions. In particular, micron-scale particles moving though viscous liquids at low Reynolds numbers ($\mathrm{Re} = \rho a U/\eta \ll 1$) acquire less charge than predicted by equation (5)[5,9] (see below). For liquid droplets, a meta-analysis of recent literature showed that droplets regularly acquire more positive than negative charge;[50] such anomalous charging behavior has been attributed to perturbations in the applied field (e.g., due to charging of dielectric surfaces).[27] Recent advances in measuring the charge acquired by particles during CCEP should help to identify and resolve remaining discrepancies between theory and experiment.[50]

Kinetics of Charging

When a charged particle approaches an oppositely biased electrode, the electric field in the particle-electrode gap increases inversely with the size of the gap δ as $E_{\max} \sim aE_0/\delta$.[5] For small gaps ($\delta \ll a$), the local field becomes much greater than the applied field, eventually exceeding the dielectric strength of the fluid. The resulting spark or microdischarge[7,51] creates a conductive pathway between the two surfaces prior to mechanical contact. For millimeter-scale particles or water drops, these discharges can be observed as flashes of visible light and are further evidenced by the formation of micron-scale craters on the electrode surface due to local melting.[51] The degradation of the electrode surface by repeated contact charging may contribute to deviations between the measured particle charge the predicted Maxwell charge. For a constant applied field, the diameter of the crater d is predicted to

scale with the particle radius a and the electrode separation L as $d \propto (qV_0)^{1/3} \propto a^{2/3}L^{1/3}$ – smaller particles produce smaller craters.[51]

The CCEP motion of micron-scale particles (e.g., $a \sim 10$ µm) is characterized by low Reynolds numbers at which the inertia of the fluid and the particle are negligible. Under these conditions, particles can approach the electrode surface, transfer charge, and move away without ever making mechanical contact with the surface (Fig. 2). This putative mechanism is supported by experimental measurements of CCEP motions and the accompanying electric current combined with detailed theoretical predictions.[5] At low Reynolds numbers, changes in the particle charge and thereby the electric force result in almost immediate changes in the particle velocity. Following the initiation of a microdischarge but prior to mechanical contact (Fig. 2b), the charge on the particle begins to relax to its new equilibrium value. Prior to reaching equilibrium, however, the electric force on the particle reverses direction, thereby increasing the surface separation and extinguishing the electric discharge. As a result, the charge on the particle is typically 60-80% less than that expected at equilibrium.[5]

Charge transfer at finite surface separations (~ 0.1 µm for a 10 µm sphere[5]) suggests that surface forces between the particle and the electrodes play a minimal role in *sustaining* CCEP motions: the particle can oscillate between the two electrodes without ever making mechanical contact with either surface. However, these forces are likely relevant in *initiating* particle motions – especially at lower voltages. To initiate CCEP motion, the electrostatic force must exceed the adhesion force (see below). Consistent with this hypothesis, we have observed that the minimum voltage required to initiate CCEP motions is greater than that required to sustain such motions.

Particle Dynamics

Once sufficiently charged, particles move in the electric field as determined by the balance of electrostatic and hydrodynamic forces and torques (Fig. 3a). The movement of the charged particle acts to redistribute charge on the electrodes, producing measurable currents in the

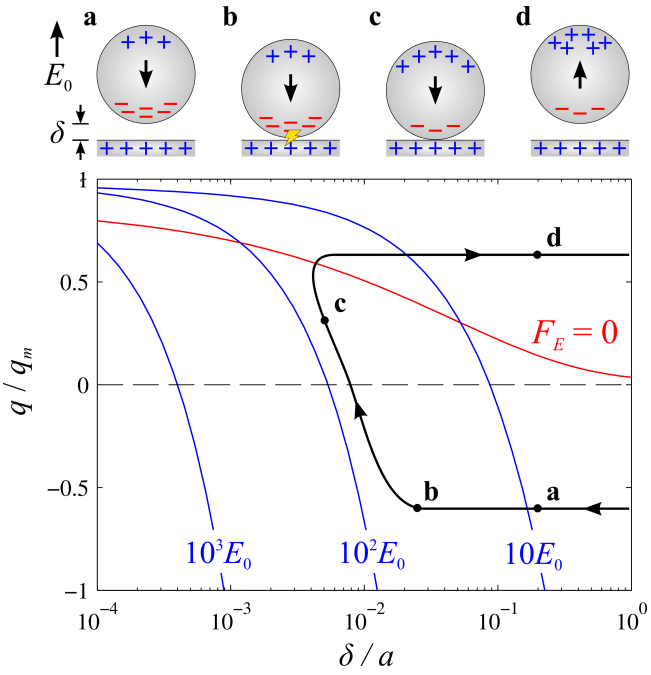

Figure 2: Qualitative particle trajectory (black) through the position-charge phase space. The surface separation δ is scaled by the particle radius a; the sphere charge q is scaled by the Maxwell charge q_m of equation (5). The blue curves show lines of constant electric field $E_{\max}$ within the sphere-electrode gap as multiples of the applied field, E_0. The red curve shows the line of zero electric force: $F_E < 0$ below the line and $F_E > 0$ above. (Adapted from reference 5; copyright 2015 American Chemical Society.)

external circuit (Fig. 3b). One distinguishing feature of CCEP motions is the asymmetry of particle-electrode "collisions". Particles approach the electrode at a near constant velocity but depart slowly, accelerating to a constant velocity on time scales of order $\eta/\varepsilon E_0$. These and other experimental trends are captured quantitatively by the following models.

Electrostatic Forces & Torques

A charged conductor in a dielectric fluid experiences an electric force $\boldsymbol{F}_E$, which can be calculated by integrating the Maxwell stress over the particle surface

$$\boldsymbol{F}_E = \int_{S_p} \frac{1}{2}\varepsilon E^2 \boldsymbol{n} dS, \tag{6}$$

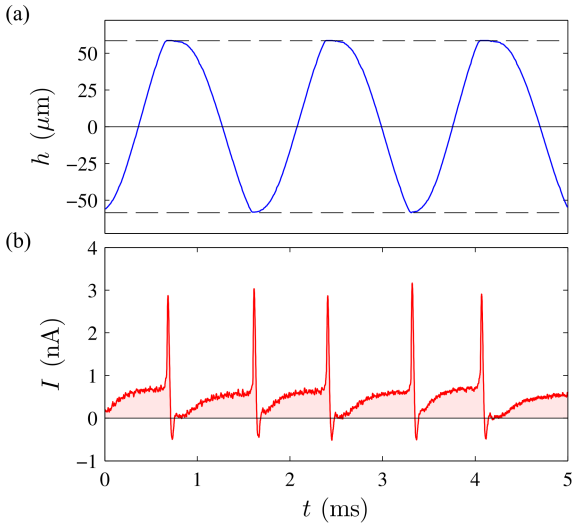

Figure 3: Synchronized particle trajectory $h(t)$ and electrical current $I(t)$ for a 28 µm sphere moving through mineral oil between two electrodes separated by a distance $L = 145$ µm and energized by a voltage $V_0 = 765$ V. (Reproduced from reference 5; copyright 2015 American Chemical Society.)

where $\boldsymbol{E} = -\nabla\phi$ is the electric field. This exact expression is often approximated by decomposing the field into two contributions: that due to charge on the particle $\boldsymbol{E}_p$ and that due to charge on the electrodes (and other particles) $\boldsymbol{E}^\infty$. By expanding the particle field in a multipole expansion, the above integral can be expanded as

$$\boldsymbol{F}_E = q\boldsymbol{E}^\infty + \boldsymbol{p}\cdot\nabla\boldsymbol{E}^\infty + \ldots, \tag{7}$$

where $\boldsymbol{p}$ is the particle dipole moment. The first two terms in the expansion correspond to the electrophoretic and dielectrophoretic forces, respectively, within an dielectric fluid.

As CCEP motions involve repeated contact between the particle and the electrodes, it is often necessary to include contributions due to higher order moments of the particle charge implicit in equation (6) to obtain an accurate description. Complete analytical solutions are available for a spherical particle near a plane electrode.[46,52,53] These solutions reveal a striking asymmetry between the approach of a charged particle to an oppositely biased electrode and its departure from that electrode after charge transfer.[47] In particular, the

force on a positively charged sphere ($q = q_m$) departing the positively biased electrode is

$$F_E = 0.832 q_m E_0 + O(\xi) \quad \text{(departing)}, \tag{8}$$

where q_m is the Maxwell charge of equation (5), and $\xi = \delta/a$ is the dimensionless surface separation.[52] The reduction in the force from the expected value of $q_m E_0$ is due to the attraction of the charged sphere to its image in the nearby electrode. By contrast, the force on a negatively charge sphere ($q = -q_m$) approaching the same positively biased electrode is

$$F_E = -\frac{6.58}{\xi f^2(\xi)} q_m E_0 + O(\ln \xi) \quad \text{(approaching)}, \tag{9}$$

where $f(\xi)$ is a slowly varying logarithmic function.[47] The force increases asymptotically with decreasing separation as ξ^{-1}. It is this asymmetry in the electrostatic force that causes the asymmetric particle trajectories observed in experiment (Fig. 3a).

Even when analytical solutions are unavailable, there exist efficient simulation techniques based on Stokesian dynamics that accurately capture both the far field and near field contributions to the electrostatic interactions.[47,54,55] Bonnecaze and Brady applied this approach to describe the electrostatics of many, spherical particles interacting in an unbounded medium.[55] More recently, we considered the case of a single sphere bounded by two plane electrodes – the prototypical CCEP geometry.[47] A logical next step is the integration of these approaches to describe the dynamics of many particles moving between two electrodes. For non-spherical particles, one must turn to more general (but less efficient) numerical methods such as finite element solvers to compute the relevant electrostatic forces.[11]

Non-spherical particles also experience an electric torque about the particle center $\boldsymbol{x}_p$ defined as

$$\boldsymbol{L}_E = \int_{S_p} \frac{1}{2} \varepsilon E^2 (\boldsymbol{x} - \boldsymbol{x}_p) \times \boldsymbol{n} dS. \tag{10}$$

To first order, this torque can be approximated as the cross product between the dipole

moment and the field,

$$\boldsymbol{L}_E = \boldsymbol{p} \times \boldsymbol{E}^\infty + \dots . \tag{11}$$

The dipole moment on a conductive particle is a linear function of the field: $\boldsymbol{p} = q(\boldsymbol{x}_q - \boldsymbol{x}_p) + \boldsymbol{\alpha} \cdot \boldsymbol{E}^\infty$, where $\boldsymbol{x}_q$ is the center of charge, and $\boldsymbol{\alpha}$ is the symmetric polarizability tensor.[39] Note that the particle center $\boldsymbol{x}_p$ (e.g., the center of hydrodynamic reaction[56]) need not coincide with the center of charge $\boldsymbol{x}_q$. Physically, particles rotate to induce the largest dipole moment aligned with the field. As discussed below, these rotational motions can serve to rectify CCEP oscillations and drive steady motions of asymmetric particles.

Hydrodynamic Drag

At low Reynolds numbers, the electrostatic forces and torques are balanced by equal and opposite hydrodynamic forces $\boldsymbol{F}_H$ and torques $\boldsymbol{L}_H$ due to motion of the particle through its viscous surroundings. Owing the linearity of the Stokes equations governing fluid motion, the hydrodynamic forces and torques are linearly related to the translational and rotational velocities of the particle(s).[57] The so-called resistance (or mobility) tensors relating these quantities depend on the position and orientation of the particle(s) relative to the bounding electrodes. In general, these tensors must be computed numerically by integrating the Stokes equations subject to no-slip conditions at the surfaces of the particle(s) and electrodes. However, there are few special geometries relevant to CCEP dynamics, for which analytical solutions and/or efficient numeric solutions are available.

Arguably, the most important case is that of a sphere moving in an unbounded fluid; the hydrodynamic drag is given by Stokes' law[58]

$$\boldsymbol{F}_H = -6\pi\eta a \boldsymbol{U}. \tag{12}$$

This expression provides a useful approximation when the particle is separated from either electrode by many particle radii. When the particle is near either electrode, the hydrody-

namic resistance increases significantly due to fluid flow into or out from the particle-electrode gap. These effects are accurately captured by analytical solutions for a solid sphere moving near a solid plane boundary.[59–62] Of particular interest is motion normal to a plane surface, for which equation (12) is modified by a multiplicative factor $\lambda(\xi)$ that depends on the surface separation $\xi = \delta/a$.[60] For small separations ($\xi \ll 1$), the resistance increases as $\lambda = \xi^{-1} + \ln(\xi)$. When a charged particle approaches contact with an electrode, the increase in the hydrodynamic resistance is almost exactly balanced by a similar increase in the electric force (see equation (9)). Upon charging, however, the electric force is greatly reduced (see equation (8)), and the particle moves slowly to escape from the electrode surface.

Even at large separations, the approach to Stokes' law occurs slowly as $\lambda = 1 + \frac{9}{8}\xi^{-1}$ due to long range hydrodynamic interactions with the wall. In general, such interactions with the bounding electrodes and other particles are not pairwise additive. Accurate treatments require efficient techniques such as Stokesian dynamics to capture the many body interactions between the particle(s) and the electrodes as well as the lubrication forces near contacting surfaces.[63–65]

Other Forces: Gravity, Inertia, Adhesion

The above analysis of particle motions neglects several forces that can be relevant to CCEP depending on the experimental conditions. The significance of these forces can be assessed by comparing their magnitude to that of the electric forces driving CCEP motions, $F_E \sim 4\pi\varepsilon a^2 E_0^2$. Forces due to gravity and inertia scale as the particle volume and are therefore significant for larger particle sizes. As an example, we consider the motion of a steel sphere ($\rho_p = 8000\ \mathrm{kg\,m^{-3}}$) in mineral oil ($\rho = 840\ \mathrm{kg\,m^{-3}}$, $\eta = 0.027\ \mathrm{Pa\,s}$, $\varepsilon = 2.5\varepsilon_0$) due to an applied field of $E_0 = 2\ \mathrm{V\,\mu m^{-1}}$. The gravitational force $F_G \sim \frac{4}{3}\pi a^3(\rho_p - \rho)g$ becomes comparable to the electric force only for millimeter-scale particles. Similarly, forces due to particle inertia $F_I \sim \frac{4}{3}\pi a^3 \rho_p U^2/a$ become significant for particle sizes of order 100 µm or larger.[9]

By contrast, forces due to surface adhesion scale with the linear dimension of the particle and are therefore significant for smaller particle sizes. In the Hamaker approximation, the van der Walls force between a sphere and a plane scales as $F_{vdW} \sim aA/6\delta^2$ where A is the Hamaker constant.[38] Continuing the example above, this force is comparable to the electric force for 10 µm particles, assuming $A = 10^{-19}$ J and $\delta = 1$ nm.[38] When the electric force is smaller than adhesive surface forces, the particle remains "stuck" to the electrode surface. A finite "lift-off" voltage is therefore required to initiate particle motion.[8,9] As the particle size decreases, larger electric fields are required to induce CCEP motions. Notably, by increasing the field to $E_0 \approx 16\ \mathrm{V\,\mu m^{-1}}$, we were able to drive the motion of a 1 µm gold sphere between two gold wires at speeds of 100 $\mathrm{mm\,s^{-1}}$ (10^5 body lengths per second). The application of larger fields is limited by the dielectric strength of the fluid; however, it may be possible to manipulate smaller particles by tailoring their surface chemistry to mitigate adhesion. Further study is required to investigate the role of surface forces in initiating and sustaining CCEP motions.

Dynamics of Anisotropic Particles

The motion of spherical particles is relatively simple due to the absence of electric torques and the symmetry of the resistance tensor. The motion of anisotropic particles is considerably more complex – even in uniform fields and unbounded fluids. Here, we discuss the dynamics of two specific particle types: a conductive rod and a Janus sphere with a conductive hemispherical cap.[11] The generalization of these specific examples to describe the motions of other particle shapes and symmetries is an interesting topic for further study.

Preferred Orientations

When subject to a uniform electric field, an uncharged conductive particle of anisotropic shape adopts a preferred orientation that maximizes the particle's dipole moment. Conductive rods rotate to align their long axis parallel to the applied field; Janus spheres rotate to

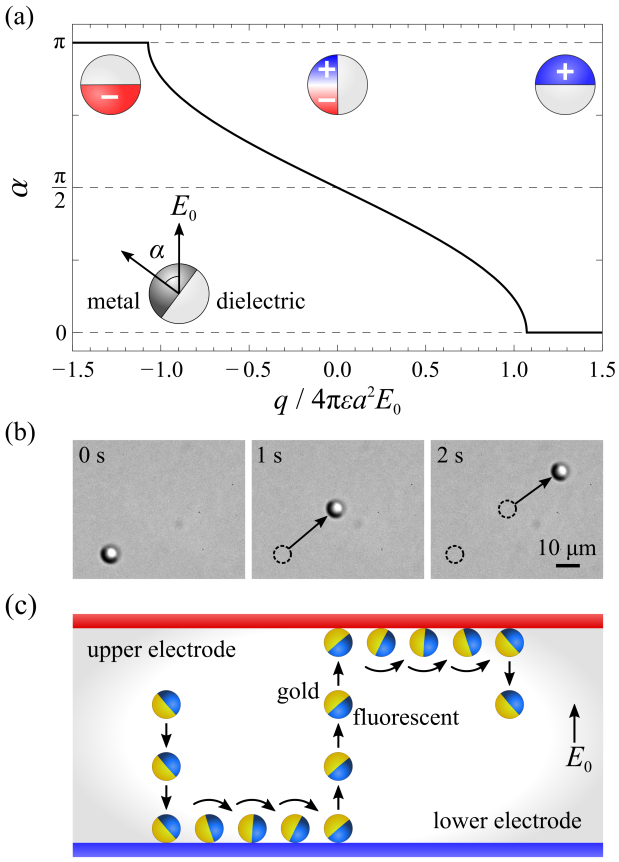

Figure 4: (a) Stable orientation α of a metallodielectric Janus sphere in a uniform electric field depends on the particle's charge q. Uncharged particles align perpendicular to applied field E_0; highly charged particles align parallel to the field. (b) Top view of a gold-silica Janus sphere oscillating between two transparent electrodes. Over many oscillation cycles, the particle moves in the direction opposite its conductive hemisphere. (c) Illustration of the propulsion mechanism showing one oscillation cycle. (Adapted from reference 11; copyright 2016 American Chemical Society.)

align their axis perpendicular to the applied field (Fig. 4a). The addition of charge to the rod does not influence its preferred orientation but causes it to move parallel to the field. In this case, the particle's center of charge and its center of hydrodynamic reaction[56] are one an the same. By contrast, the center of charge on the Janus particle is displaced from the center of the sphere towards the conductive cap. As a result, the addition of charge to the Janus sphere alters its dipole moment an thereby its preferred orientation. Figure 4a shows the stable orientation of the Janus particle as a function of the charge q on its conductive hemisphere. Importantly, the dipole moment due to charge acquired by contact charging is

comparable to that due to polarization (i.e., $qa \sim p$ when $q \sim 4\pi\varepsilon a^2 E_0$ and $p \sim 4\pi\varepsilon a^3 E_0$).[40] As a result, the particle adopts a stable orientation with its axis oblique to the applied field. Moreover, as the particle oscillates between two electrodes, its orientation also oscillates between two stable values.

Rectified Motions

CCEP oscillations of Janus particles between parallel electrodes are accompanied by steady motions directed perpendicular to the applied field[11] (Fig. 4b). These lateral motions are caused by successive particle rotations following each charge transfer at the electrode surface (Fig. 4c). Each time the particle contacts an electrode, its charge changes sign, thereby altering its preferred orientation in the field. The field-induced rotation of the particle in the vicinity of the electrode surface results in a lateral displacement, which is qualitatively similar to that of a sphere "rolling" along the surface. Successive rotations occur in a common direction toward the nonmetallic hemisphere, causing a steady motion over the course of many oscillations. This mechanism is supported both by experiments with fluorescent particles that reveal their rotational motions and by simulations of CCEP dynamics that capture the electrostatic and hydrodynamic forces and torques outlined above. This strategy for rectifying particle oscillations to achieve directed motion is not limited to Janus spheres. Similar motions are observed for other anisotropic particles (e.g., clusters of spherical particles); however, further work is needed to understand and optimize particle shapes to maximize directed motion.

Dynamics of Multiple Particles

The vast majority of CCEP studies have focused on the dynamics of individual particles, and there remains much to explore when many particles move and interact with one another. Particles interact over large distances through both electrostatic and hydrodynamic forces. Additionally, particle "collisions" can serve to redistribute charge among particles in contact.

To date, these effects have been shown to guide the formation of dynamic chains (so-called bucket brigades[66]), the synchronization of neighboring oscillators,[67] and the emergence of collective motions.[11]

Bucket Brigades

The phrase "bucket brigade" refers to a method of transporting items wherein items are passed from one stationary member of the "brigade" to the next. A conceptually similar behavior occurs during CCEP of multiple particles, which organize to pass charge from one electrode to the other. In one realization, multiple aluminum discs were distributed randomly on the surface of a dielectric liquid between two electrodes (Fig. 5a).[66] Upon application of the field, the discs organized to form linear chains which oscillated continuously passing charge from neighbor to neighbor. Similar behaviors have been observed for water drops moving in oil between two electrodes.[14] Importantly, the number of particles in the chain cannot exceed $L/2a$; otherwise, they will span the gap between the electrode and short the circuit.

We have observed similar chains of spheres moving in mineral oil between two electrodes. Interestingly, particles appear to collide "elastically" despite the absence of inertia at low Reynolds numbers (Fig. 5b). During a collision between two spheres, the total charge is conserved and redistributes between the spheres to achieve a common electric potential. The amount of charge acquired during a sphere-sphere collision is the same as that acquired by contact with either electrode.[40,68] These dynamical behaviors are well captured by Stokesian dynamics simulations of CCEP motions that incorportate the electrostatic and hydrodynamic contributions detailed above.

Synchronization

Prior to the formation bucket brigades, neighboring particles moving by CCEP begin to oscillate with a common frequency – that is, they synchronize.[67] Unlike many types of coupled

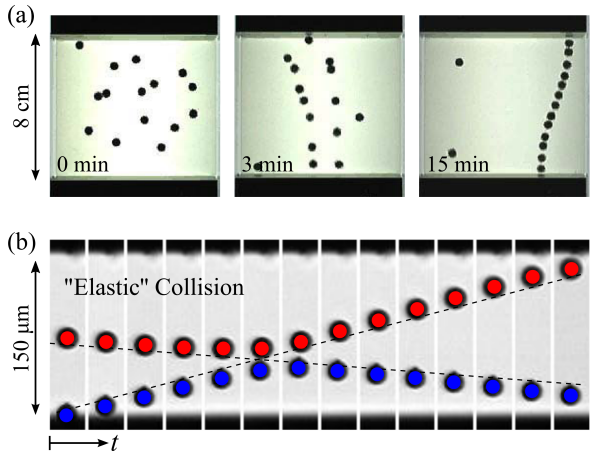

Figure 5: (a) Dynamic formation of a "bucket brigade" of aluminum disks in a $E_0 = 0.3$ V µm^{-1} field. (Reproduced from reference 66; copyright 2014 IEEE Computer Society.) (b) Successive images of two spheres colliding "elastically" at lows Reynolds numbers; the time between successive images is 40 ms.

oscillators which move in phase, CCEP oscillators prefer to move in an anti-synchronous fashion with a phase difference of 180°. As a result, the two particles always have charge of opposite polarity and attract one another. These synchronized Coulombic interactions along with dipole-dipole forces are ultimately responsible for the organization of dynamic particle chains. Unfortunately, the synchronization of dynamic assemblies by CCEP is limited by the particles' propensity to form chains that span the electrodes and short the circuit. Short circuits can be eliminated by constraining particle motions along dielectric "tracks", which do not interfere with the electrostatic interactions driving synchronization. The exploration of synchronization and dynamic pattern formation among CCEP oscillators is exciting direction for further study – both for its interesting physics and its potential relevance in coordinating the motions of many particles for useful functions (see below).

Microfluidic Applications

The attributes of contact charge electrophoresis make it potentially attractive for powering the active unit operations of microfluidic devices using portable battery power. Despite their

small size, "lab-on-a-chip" (LoC) devices are often accompanied by bulky external equipment used for fluid transport,[69] mixing,[70] and detection.[71] This lack of self-containment can limit the use of LoC devices in point-of-care diagnostic systems, which seek to address health care challenges in regions without centralized medical facilities.[20,21] The development of mobile microfluidic platforms for fast, accurate, and inexpensive medical diagnostics remains an important challenge for global health.[72] To help address this need, we have developed CCEP-based systems for rapid particle transport,[4,73] separations,[4] and fluid mixing.[10] These demonstrations motivate the pursuit of other microfluidic operations such as pumping fluids and controlling heat/mass transfer via CCEP motions.

We note that the low power requirements of CCEP do not imply low voltage operation directly accessible by standard battery technologies. The unit operations below rely on relatively high voltages (typically, $10^2 - 10^3$ V) to achieve maximum performance. Such voltages are readily supplied by miniature, battery-powered amplifiers,[74] which are ca. 1 cm^3 in size and commercially available. These amplifiers are commonly used to improve the performance of on-chip electrophoretic separations which benefit from high voltages ($\sim 10^3$ V) but require little current ($\sim$1 μA, as in capillary electrophoresis[75]).

Ratcheted Transport

Most studies of CCEP have been limited to simple oscillatory motions between two electrodes. To realize the full potential of this mechanism (e.g., for particle transport or droplet manipulation), effective strategies are required for rectifying particle oscillations to achieve directed linear or rotational motions.

We developed one such strategy that uses ratcheted microfluidic channels to direct CCEP motions perpendicular to the applied field.[4] As illustrated in Figure 6, the oscillatory motion of a conductive particle between two parallel electrodes can be biased by a series of inclined dielectric barriers ("teeth") that translate the electric force in the "vertical" direction into directed motion along the "horizontal" direction. This microfluidic ratchet is fabricated in

polydimethylsiloxane (PDMS) using soft lithography.[76] To create electrodes that connect directly to the center channel, we flow liquid gallium (at 40°C) into the electrode channels using capillarity to prevent flow into the center channel.[77] After cooling to solidify the electrodes, we flow in particles suspended in mineral oil, apply a DC voltage between the two electrodes, and monitor the motion of the particles using a high speed camera. Remarkably, this CCEP ratchet allows for rapid particle transport (velocities of few cm s^{-1}) over arbitrary distances using DC voltages and very low power (typically, ~1 nW). By contrast, DEP requires complex electric fields that vary in space and time (e.g., traveling wave DEP[78,79]) to achieve comparable performance.

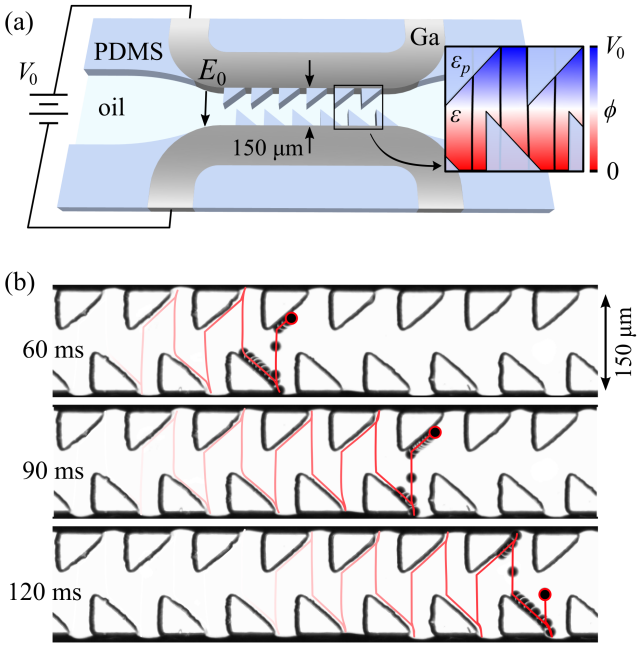

Figure 6: (a) Ratcheted microfluidic channel for directed particle transport. As the dielectric constant of PDMS is similar to that of mineral oil, the applied electric field remains nearly uniform throughout the interelectrode region (inset). (b) Reconstructed particle trajectories show the directed motion of a single 20 µm particle (silver coated glass sphere) for $E_0 = 4.6$ V µm^{-1}. Each image is a composite of 16 individual frames collected at intervals of 0.67 ms; the position of the shuttle at each of those 16 time points is denoted by the black circle. The red line traces the shuttles trajectory in time. The speed of the particle through the fluid is 50,000 µm s^{-1}; the average speed of the particle in the horizontal direction is 5,000 µm s^{-1}. (Reproduced from reference 4 with permission of The Royal Society of Chemistry.)

The same approach also enables the rapid transport of hydrogel capsules and aqueous

droplets, which can serve as containers for chemical and biological cargo. We recently described how CCEP can be used both to generate and transport aqueous droplets within a microfluidic system powered by a single, constant voltage input.[73] Drop generation is achieved through an electrohydrodynamic dripping mechanism by which conductive drops grow and detach from a grounded nozzle in response to an electric field. The now-charged drops are then transported down the ratcheted channel by CCEP in a manner similar to that of solid particles. By contrast, however, drops can deform in response to electric stresses acting at their surface. Such deformations are opposed by surface tension, which favors spherical drops that minimize the interfacial area. Ratcheted transport of drops requires sufficiently small capillary numbers (typically, $\mathrm{Ca} = \varepsilon E_0^2 a/\gamma < 1$), which limits the magnitude of the applied field and thereby the speed of drop transport.

Separations

The use of dielectric barriers to direct CCEP motions can be generalized to perform other functions such as separating and collecting particles.[4] This approach is illustrated in Figure 7, which shows a ratcheted microfluidic system for the separation of particles from a fluid stream. In the design process, we start with the desired functionality – particles will enter from channel 1 and exit from channel 2 – and choose the positon and polarity of the electrodes to ensure that the particle will only oscillate in the appropriate channels (e.g., not in channel 3; Fig. 7a). We then calculate the electric field between the electrodes for the proposed geometry using a finite element solver (Fig. 7b). Provided the dielectric constants of the PDMS barriers are similar to that of the fluid, the electric field lines will not be affected by the placement of the dielectric teeth.

The design of the dielectric barriers is guided by three heuristic rules for predicting particle motions: (i) a particle moves along the electric field lines until it contacts a surface, (ii) it slides / rolls along inclined dielectric barriers, and (iii) it reverses direction when it contacts an electrode surface. The key function of the dielectric barriers is to move a

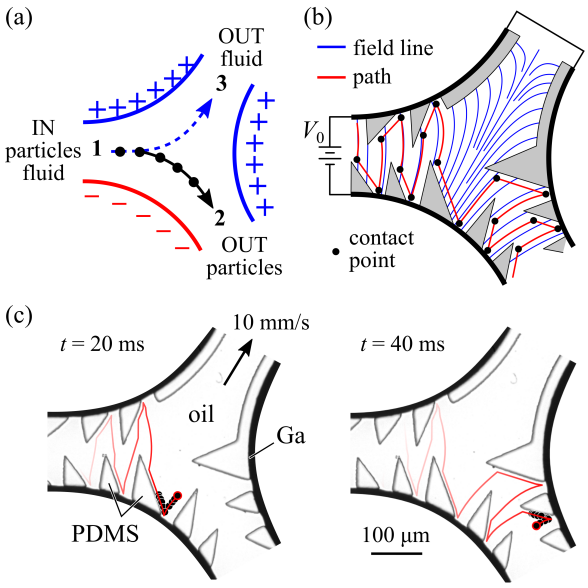

Figure 7: (a) Ratcheted CCEP system for separating particles from a fluid stream. (b) Schematic illustration showing the dielectric barriers (grey), electrodes (black), electric field lines (blue), and the anticipated particle trajectory (red). (c) Experimental realization of this design showing the dynamics of a 20 µm particle. The red line shows the reconstructed particle trajectory; the black circles denote the position of the particle at regular intervals of 0.2 ms. (Reproduced from reference 4 with permission of The Royal Society of Chemistry.)

charged particle from one field line to another in programmed manner. With these rules, the PDMS teeth are designed by tracing field lines and adding barriers to direct particle motion. Implementing the design in a microfluidic system (Fig. 7c), we find remarkable agreement between the actual particle motion and that predicted by the simple heuristics.[4]

Importantly, the rapid motion of particles via CCEP ($\sim$100 mm s^{-1}) effectively decouples their motion from that of the surrounding fluid ($\sim$1 mm s^{-1}); this enables particles to be transported upstream or downstream regardless of fluid flow.[4] Looking forward, we envision the development of CCEP-based transport systems for several useful applications including (i) the recycling of high-value catalyst particles in microfluidic reactors through "upstream" particle transport, (ii) capture and accumulation of particles in dead-end channels for isolation and analysis, as well as (iii) transport, manipulation, and merging of microfluidic droplets.

Mixing

The programmed transport of micron-scale particles within microfluidic systems can also be harnessed to rapidly mix laminar streams. Mixing two or more fluids within a microfluidic device can be challenging due to the absence of turbulence at low Reynolds numbers.[80,81] Within laminar flows, mixing is achieved through molecular diffusion, which requires a characteristic time $\tau \sim \ell^2/D$ to homogenize the fluid composition over a length scale ℓ (here, D is the diffusion coefficient). Effective mixers act to stretch and fold the flowing streams to reduce the length over which diffusion must act and accelerate the rate of diffusive mixing. Active microfluidic mixing using applied electric fields is often achieved through electrohydrodynamic flows[82,83] caused by the action of the field on ionic space charge. While effective in aqueous systems, electrohydrodynamic mixers do not function in most organic fluids due to the absence of dissolved ions. By contrast, CCEP enables the rapid oscillatory movement of particles through dielectric fluids. These particle motions can be applied to mix organic liquids, which are used in the context of combinatorial syntheses and drug discovery.[84,85]

Figure 8 illustrates a simple mixer designed to mix two laminar streams.[10] Application of a DC voltage to the gallium electrodes creates a non-homogeneous electric field that enables the dielectrophoretic capture of a conductive particle, which then oscillates between the electrodes via CCEP. Perhaps surprisingly, we found that linear particle motions perpendicular to the direction of flow does not result in effective mixing due to the kinematic reversibility of low-Reynolds number flows.[41,86] The mixing achieved by the "upward" movement of the particle is almost entirely reverse by its "downward" motion. By contrast, orbital particle motions guided by dielectric barriers (analogous to those used in the ratchets of the previous section) break the time-reversal symmetry and allow for effective mixing over lengths comparable to the width of the channel. Complete mixing requires that the speed of the particle be much larger than the fluid velocity such that the particle completes many orbits as the fluid flows through the mixing region. The extent of mixing also depends strongly on the size of the particle and the shape of its trajectory; effective mixers relied on larger particles

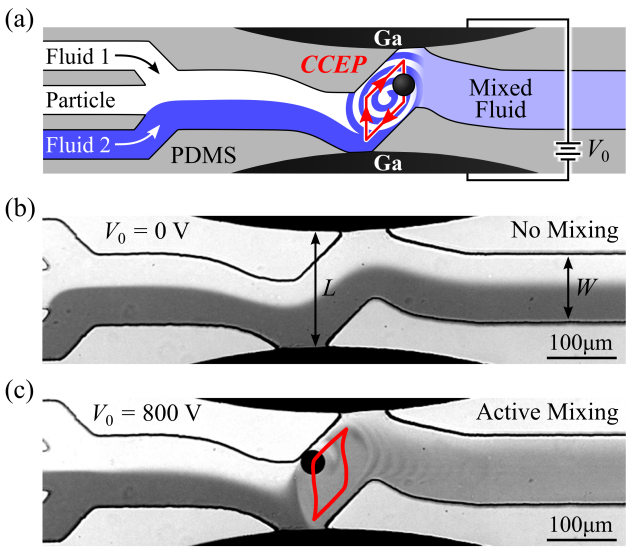

Figure 8: Schematic illustration of a microfluidic mixer based on CCEP. Two dielectric fluids (here, mineral oil with and without dye) flow laminarly into the channel and are mixed by the orbital motion of the particle. (b) Image of the mixer before introducing the particle and applying the electric field; the average fluid velocity is $u \approx 1\ \mathrm{mm\,s^{-1}}$. (c) Application of a constant voltage drives the oscillatory motion of the particle, which thoroughly mixes the two streams. The red curve denotes the particle trajectory. (Reproduced from reference 10 with permission of The Royal Society of Chemistry.)

(comparable to the size of the channel) moving along non-reciprocal orbits.

Future Directions

Contact charge electrophoresis is a promising technique for the electric manipulation of micron-scale particles and droplets. There remain outstanding opportunities to advance both our fundamental understanding of CCEP and our ability to apply it for microfluidic systems. More broadly, we recognize two frontiers for CCEP research: one based on further miniaturization to sub-micron dimensions, another based on the integration of many CCEP oscillators to form active, macroscopic materials. We close with a discussion of these complementary pursuits.

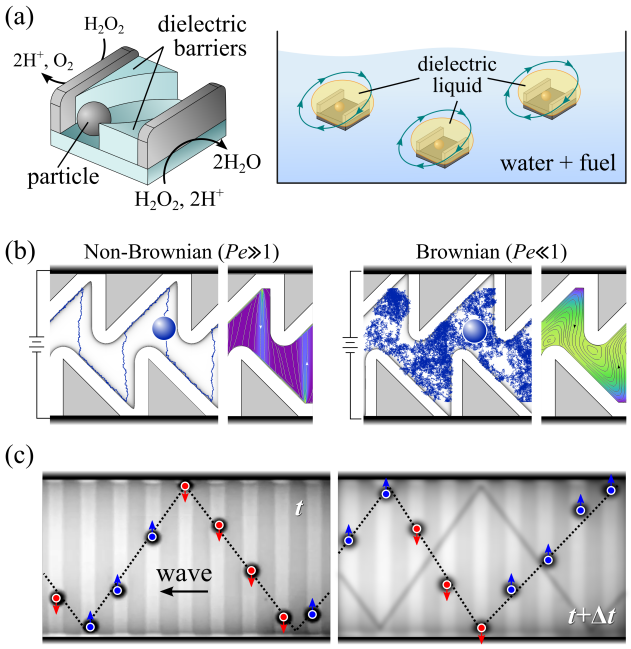

Figure 9: (a) Illustration of chemically powered, active emulsion droplets powered by CCEP. (b) Ratcheted CCEP transport is effective even at low Péclet numbers, $\mathrm{Pe} = aF_e/k_BT \ll 1$. Blue curves show individual particle trajectories; the colormaps and streamlines show the steady-state particle density and flux, respectively. (Reproduced from reference 87; copyright 2016 AIP Publishing LLC). (c) Electrostatically coupled CCEP oscillators synchronize to form traveling waves capable of transport and actuation.

Go Smaller

Our study of CCEP was originally inspired by the catalytic nanomotors of Sen and Mallouk, who showed how electrochemical reactions could be harnessed to power the autonomous motion of colloidal particles.[88] Using catalytic materials, these nanoscale machines convert chemical energy from their surrounding environment into steady electric currents that lead to self-electrophoresis of the particles.[89] Importantly, only a tiny fraction of the chemical energy used is converted into the fluid flows that drive particle motions.[90] In this context, CCEP may provide an efficient electric motor, with which to realize the potential of chemically-powered colloidal machines. Of course, there remain many fundamental and technical challenges that must first be overcome.

CCEP motions described in the sections above were powered by large voltages – significantly greater than that provided by a single electrochemical reaction (ca. $0.1-1$ V). Rapid

particle motions are possible at these smaller voltages provided the electrode separation is also reduced to maintain large electric fields (ca. 1 $\mathrm{V\,\mu m^{-1}}$). Perhaps the greater challenge is preventing particle adhesion at the electrodes, which becomes increasingly problematic at smaller scales (see above). There are two main strategies for reducing adhesive forces: change the surface chemistry and/or reduce the contact area. For example, by coating both the electrodes and the particle with a self-assembled monolayer of 1-octadecanethiol, we observed that the lift-off voltage for CCEP motion was reduced by a factor of $\sim$5. It is desirable to identify molecular surface coatings that both reduce adhesion forces and allow facile charge transfer on contact. Additionally, one can modify the geometry of the particle and/or electrode to reduce the contact area without significantly altering the electric forces driving CCEP motions. So-called "hedgehog particles" with an armor of rigid spikes are a particularly attractive candidate to investigate.[91]

Another challenge is linking CCEP motions in dielectric fluids to autonomous functions in aqueous environments. One possible approach is to embed CCEP motors within emulsion droplets and rely on the hydrodynamic coupling of particle motions inside the drop to drive external flows (Fig. 9a). Such active droplets could convert chemical energy into motion with efficiency improvements of up to seven orders of magnitude over existing motors.[90] Dramatic improvements in the energy efficiency of colloidal machines could enable their autonomous operation in low fuel environments. In addition to improved efficiency, ratcheted transport using CCEP is predicted to be remarkably robust to Brownian motion.[87] Buffeted by an incessant assault of thermal noise, nanoscale ratchets continue to function effectively, in sharp contrast other ratcheting mechanisms (Fig. 9b).

Go Bigger

At the other end of the spectrum, the collective motions of many CCEP oscillators may provide a basis for soft actuator materials inspired by biological muscle. Muscles are motors: they convert chemical free energy into mechanical motion and generate large forces through

the steady repetition of small steps namely, those of myosin motor proteins. By orchestrating the coordinated action of these many elemental motors, living organisms perform a diverse range of mechanical functions. Similarly, the electrostatic and hydrodynamic interactions among arrays of CCEP oscillator can lead to self-organized motions such as traveling wave synchronization (Fig. 9c). The distributed actuation of many CCEP oscillators can be harnessed to perform useful mechanical functions such as cargo transport and locomotion.

In particular, the fabrication of oscillator arrays in soft, elastomeric materials could provide a basis for new types of actuator materials – so-called artificial muscles. Soft materials are readily deformed by electric stresses, which can vary in time due to motions of charged particles. In this way, traveling waves of particle motion can be translated into traveling waves of material deformation. Such self-organized deformations are potentially useful for driving the locomotion of soft robots (e.g., inchworm-type motions) at the scale of microns to millimeters.[92,93] Like biological muscle, active materials based on many elemental actuators are robust to failure of individual components and allow for complex collective motions.

Coda

From its humble beginnings more than 250 years ago, the electrostatic motor and its colloidal analogs are well positioned to contribute to a new industrial revolution at the micro- and nanoscales. The realization of active microfluidic systems and colloidal machines[94] that organize in space and time to perform useful functions requires efficient mechanisms for converting energy into motion. Applied creatively, contact charge electrophoresis can be engineered to power an increasingly diverse set of mechanical operations that meets these needs.

Acknowledgement

This work was supported by National Science Foundation Grant CBET 1351704.

References

(1) Potamian, F.; Walsh, J. *Makers of Electricty*; Fordham University Press: New York, 1909; pp 68–132.

(2) Franklin, B. In *The Collected Papers of Benjamin Franklin*; Labaree, L., Ed.; Yale University: New Haven, 1962; Chapter 5, p 69.

(3) Franklin, B. *Experiments And Observations On Electricity*; E. Cave: London, 1751; pp 28–29.

(4) Drews, A. M.; Lee, H.-Y.; Bishop, K. J. M. Ratcheted electrophoresis for rapid particle transport. *Lab Chip* **2013**, *13*, 4295–4298.

(5) Drews, A. M.; Cartier, C. A.; Bishop, K. J. M. Contact Charge Electrophoresis: Experiment and Theory. *Langmuir* **2015**, *31*, 3808–3814.

(6) Krotkov, R. V.; Tuominen, M. T.; Breuer, M. L. Franklin's Bells and charge transport as an undergraduate lab. *Am. J. Phys.* **2001**, *69*, 50.

(7) Tobazeon, R. Electrohydrodynamic behaviour of single spherical or cylindrical conducting particles in an insulating liquid subjected to a uniform DC field. *J. Phys. D: Appl. Phys.* **1996**, *29*, 2595–2608.

(8) Khayari, A.; Perez, A. Charge aquired by a spherical ball bouncing on an electrode: Comparison between theory and experiment. *IEEE Trans. Dielectr. Electr. Insul.* **2002**, *9*, 589–595.

(9) Knutson, C. R.; Edmond, K. V.; Tuominen, M. T.; Dinsmore, A. D. Shuttling of charge by a metallic sphere in viscous oil. *J. Appl. Phys.* **2007**, *101*, 13706.

(10) Cartier, C. A.; Drews, A. M.; Bishop, K. J. M. Microfluidic Mixing of nonpolar liquids by contact charge electrophoresis. *Lab Chip* **2014**, *14*, 4230–4236.

(11) Dou, Y.; Cartier, C.; Fei, W.; Pandey, S.; Razavi, S.; Kretzschmar, I.; Bishop, K. Directed motion of metallodielectric particles by contact charge electrophoresis. *Langmuir* **2016**, *32*, 13167–13173.

(12) Hase, M.; Watanabe, S. N.; Yoshikawa, K. Rhythmic motion of a droplet under a dc electric field. *Phys. Rev. E* **2006**, *74*, 46301.

(13) Jung, Y.-M.; Oh, H.-C.; Kang, I. S. Electrical charging of a conducting water droplet in a dielectric fluid on the electrode surface. *J. Colloid Interface Sci.* **2008**, *322*, 617–623.

(14) Ristenpart, W. D.; Bird, J. C.; Belmonte, A.; Dollar, F.; Stone, H. A. Non-coalescence of oppositely charged drops. *Nature* **2009**, *461*, 377–380.

(15) Jung, Y. M.; Kang, I. S. A novel actuation method of transporting droplets by using electrical charging of droplet in a dielectric fluid. *Biomicrofluidics* **2009**, *3*, 22402.

(16) Im, D. J.; Noh, J.; Moon, D.; Kang, I. S. Electrophoresis of a charged droplet in a dielectric liquid for droplet actuation. *Anal. Chem.* **2011**, *83*, 5168–5174.

(17) Ahn, B.; Lee, K.; Panchapakesan, R.; Oh, K. W. On-demand electrostatic droplet charging and sorting. *Biomicrofluidics* **2011**, *5*, 24113.

(18) Im, D. J.; Ahn, M. M.; Yoo, B. S.; Moon, D.; Lee, D. W.; Kang, I. S. Discrete Electrostatic Charge Transfer by the Electrophoresis of a Charged Droplet in a Dielectric Liquid. *Langmuir* **2012**, *28*, 11656–11661.

(19) Im, D. J.; Yoo, B. S.; Ahn, M. M.; Moon, D.; Kang, I. S. Digital electrophoresis of charged droplets. *Anal. Chem.* **2013**, *85*, 4038–4044.

(20) Gervais, L.; de Rooij, N.; Delamarche, E. Microfluidic chips for Point-of-Care immunodiagnostics. *Adv. Mater.* **2011**, *23*, H151–H176.

(21) Gubala, V.; Harris, L. F.; Ricco, A. J.; Tan, M. X.; Williams, D. E. Point of Care diagnostics: status and future. *Anal. Chem.* **2012**, *84*, 487–515.

(22) Birlasekaran, S. The measurement of charge on single particles in transformer oil. *IEEE Trans. Electr. Insul.* **1991**, *26*, 1094–1103.

(23) Gorelik, L. Y.; Isacsson, A.; Voinova, M. V.; Kasemo, B.; Shekhter, R. I.; Jonson, M. Shuttle Mechanism for Charge Transfer in Coulomb Blockade Nanostructures. *Phys. Rev. Lett.* **1998**, *80*, 4526–4529.

(24) Tuominen, M. T.; Krotkov, R. V.; Breuer, M. L. Stepwise and hysteretic transport behavior of an electromechanical charge shuttle. *Phys. Rev. Lett.* **1999**, *83*, 3025–3028.

(25) Mochizuki, T.; Mori, Y. H.; Kaji, N. Bouncing motions of liquid drops between tilted parallel-plate electrodes. *AIChE J.* **1990**, *36*, 1039–1045.

(26) Eow, J. S.; Ghadiri, M.; Sharif, A. Experimental studies of deformation and break-up of aqueous drops in high electric fields. *Colloids Surf., A* **2003**, *225*, 193–210.

(27) Yang, S. H.; Im, D. J. Electrostatic Origins of the Positive and Negative Charging Difference in the Contact Charge Electrophoresis of a Water Droplet. *Langmuir* **2017**, *33*, 13740–13748.

(28) Hamlin, B. S.; Ristenpart, W. D. Transient reduction of the drag coefficient of charged droplets via the convective reversal of stagnant caps. *Phys. Fluids* **2012**, *24*, 012101.

(29) Link, D. R.; Grasland-Mongrain, E.; Duri, A.; Sarrazin, F.; Cheng, Z.; Cristobal, G.; Marquez, M.; Weitz, D. A. Electric Control of Droplets in Microfluidic Devices. *Angew. Chem. Int. Ed.* **2006**, *45*, 2556–2560.

(30) Im, D. J. Next generation digital microfluidic technology: Electrophoresis of charged droplets. *Korean J. Chem. Eng.* **2015**, *32*, 1001–1008.

(31) Jones, L.; Makin, B. Measurement of charge transfer in a capacitive discharge. *IEEE Trans. Ind. Appl.* **1980**, *1A-16*, 76–79.

(32) Im, D. J.; Noh, J.; Yi, N. W.; Park, J.; Kang, I. S. Influences of electric field on living cells in a charged water-in-oil droplet under electrophoretic actuation. *Biomicrofluidics* **2011**, *5*, 44112.

(33) Gacek, M. M.; Berg, J. C. The role of acid-base effects on particle charging in apolar media. *Adv. Colloid Interface Sci.* **2015**, *220*, 108–123.

(34) Lee, J.; Zhou, Z. L.; Behrens, S. H. Charging Mechanism for Polymer Particles in Nonpolar Surfactant Solutions: Influence of Polymer Type and Surface Functionality. *Langmuir* **2016**, *32*, 4827–4836.

(35) Prieve, D. C.; Yezer, B. A.; Khair, A. S.; Sides, P. J.; Schneider, J. W. Formation of Charge Carriers in Liquids. *Adv. Colloid Interface Sci.* **2017**, *244*, 21–35.

(36) Baytekin, H. T.; Patashinski, A. Z.; Branicki, M.; Baytekin, B.; Soh, S.; Grzybowski, B. A. The Mosaic of Surface Charge in Contact Electrification. *Science* **2011**, *333*, 308–312.

(37) Garg, A.; Cartier, C. A.; Bishop, K. J.; Velegol, D. Particle Zeta Potentials Remain Finite in Saturated Salt Solutions. *Langmuir* **2016**, *32*, 11837–11844.

(38) Israelachvili, *Intermolecular and Surface Forces*, 2nd ed.; Academic Press, 1991; pp 176–178.

(39) Landau, L. D.; Lifshitz, E. *Electrohydrodynamics of continuous media*; Elsevier: NY, New York, 1984; pp 3–7.

(40) Jackson, J. D. *Classical Electrodynamics*, 3rd ed.; Wiley: New York, 1999; pp 62–64.

(41) Happel, J. R.; Brenner, H. *Low Reynolds Number Hydrodynamics*; M. Nijhoff: The Hague, 1983.

(42) Kim, D. S.; Lee, S. H.; Kwon, T. H.; Ahn, C. H. A serpentine laminating micromixer combining splitting/recombination and advection. *Lab Chip* **2005**, *5*, 739–747.

(43) Maxwell, J. *A Treatise on Electricity and Magnetism*; Oxford: Clarendon Press, 1873.

(44) Smythe, W. *Static and Dynamic Electricity*; McGraw-Hill: New York, 1950; p 121.

(45) Felici, N. J. Forces and charges of small objects in contact with an electrode subjected to an electric field. *Revue Generale de l'electricite* **1966**, *75*, 1145–1160.

(46) Davis, M. H. Two charged spherical conductors in a uniform electric field: forces and field strength. *Quarterly Journal of Mechanics and Applied Mathematics* **1964**, *17*, 499–511.

(47) Drews, A. M.; Kowalik, M.; Bishop, K. J. Charge and force on a conductive sphere between two parallel electrodes: A Stokesian dynamics approach. *J. Appl. Phys* **2014**, *116*, 074903.

(48) Cho, A. Y. H. Contact charging of micron-sized particles in intense electric fields. *J. Appl. Phys.* **1964**, *35*, 2561–2564.

(49) Colver, G. M. Dynamic and stationary charging of heavy metallic and dielectric particles against a conducting wall in the presence of a dc applied electric field. *J. Appl. Phys.* **1976**, *47*, 4839–4849.

(50) Elton, E. S.; Tibrewala, Y.; Rosenberg, E. R.; Hamlin, B. S.; Ristenpart, W. D. Measurement of Charge Transfer to Aqueous Droplets in High Voltage Electric Fields. *Langmuir* **2017**, 10.1021/acs.langmuir.7b03375.

(51) Elton, E.; Rosenberg, E.; Ristenpart, W. Crater Formation on Electrodes during Charge Transfer with Aqueous Droplets or Solid Particles. *Phys. Rev. Lett.* **2017**, *119*, 094502.

(52) Smith, G. S.; Barakat, R. Electrostatics of two conducting spheres in contact. *Appl. Sci. Res.* **1975**, *30*, 418–432.

(53) Jeffrey, D. J.; Van Dyke, M. The Temperature Field or Electric Potential Around Two Almost Touching Spheres. *J. Inst. Math. its Appl.* **1978**, *22*, 337–351.

(54) Brady, J. F.; Bossis, G. Stokesian dynamics. *Annu. Rev. Fluid Mech.* **1988**, *20*, 111–157.

(55) Bonnecaze, R. T.; Brady, J. F. A method for determining the effective conductivity of dispersions of particles. *Proc. R. Soc. A* **1990**, *430*, 285–313.

(56) Brenner, H. The Stokes resistance of an arbitrary particle. 2. An extension. *Chem. Eng. Sci.* **1964**, *19*, 599–629.

(57) Kim, S.; Karrila, S. J. *Microhydrodynamics*; Dover: Mineola, NY, 2005.

(58) Stokes, G. On the effect of the internal friction of fluids on the motion of pendulums. *Trans. Cambridge Philos. Soc.* **1851**, *9*, 8.

(59) Jeffrey, G. B.; Jeffery, G. B. On the steady rotation of a solid of revolution in a viscous fluid. *Proc. London Math. Soc.* **1915**, *14*, 327–338.

(60) Brenner, H. The slow motion of a sphere through a viscous fluid towards a plane surface. *Chem. Eng. Sci.* **1961**, *16*, 242–251.

(61) O'Neill, M. E. A slow motion of viscous liquid caused by a slowly moving solid sphere. *Mathematika* **1964**, *11*, 67–74.

(62) Dean, W. W.; O'Neill, M. M. A slow motion of viscous liquid caused by the rotation of a solid sphere. *Mathematika* **1963**, *10*, 13–24.

(63) Swan, J. W.; Brady, J. F. Simulation of hydrodynamically interacting particles near a no-slip boundary. *Phys. Fluids* **2007**, *19*, 113306.

(64) Swan, J. W.; Brady, J. F. Particle motion between parallel walls: hydrodynamics and simulation. *Phys. Fluids* **2010**, *22*, 103301.

(65) Swan, J. W.; Brady, J. F. The hydrodynamics of confined dispersions. *J. Fluid Mech.* **2011**, *687*, 254–299.

(66) Pelesko, J. A. A self-organizing bucket brigade. 2004 International Conference on MEMS, NANO and Smart Systems. Los Alamitos, 2004; pp 212–217.

(67) Mersch, E.; Vandewalle, N. Antiphase synchronization of electrically shaken conducting beads. *Phys Rev E* **2011**, *84*.

(68) Davis, M. H. Electrostatic Field and Force on a Dielectric Sphere near a Conducting PlaneA Note on the Application of Electrostatic Theory to Water Droplets. *Am. J. Phys.* **1969**, *37*, 26.

(69) Laser, D. J.; Santiago, J. G. A review of micropumps. *J. Micromech. Microeng.* **2004**, *14*, R35–R64.

(70) Nguyen, N.-T. *Micromixers: fundamentals, design, and fabrication*, 2nd ed.; William Andrew, 2012.

(71) Malic, L.; Brassard, D.; Veres, T.; Tabrizian, M. Integration and detection of biochemical assays in digital microfluidic LOC devices. *Lab Chip* **2010**, *10*, 418–431.

(72) Varmus, H.; Klausner, R.; Zerhouni, E.; Acharya, T.; Daar, A. S.; Singer, P. A. Grand challenges in global health. *Science* **2003**, *302*, 398–399.

(73) Cartier, C.; Graybill, J.; Bishop, K. Electric generation and ratcheted transport of contact-charged drops. *Phys. Rev. E* **2017**, *96*, 043101.

(74) Erickson, D.; Sinton, D.; Li, D. A miniaturized high-voltage integrated power supply for portable microfluidic applications. *Lab Chip* **2004**, *4*, 87–90.

(75) Garcia, C. D.; Liu, Y.; Anderson, P.; Henry, C. S. Versatile 3-channel high-voltage power supply for microchip capillary electrophoresis. *Lab Chip* **2003**, *3*, 324–328.

(76) Xia, Y. N.; Whitesides, G. M. Soft lithography. *Annu. Rev. Mater. Sci.* **1998**, *28*, 153–184.

(77) So, J.-H.; Dickey, M. D. Inherently aligned microfluidic electrodes composed of liquid metal. *Lab Chip* **2011**, *11*, 905–911.

(78) Hagedorn, R.; Fuhr, G.; Muller, T.; Gimsa, J. Traveling-wave dielectrophoresis of microparticles. *Electrophoresis* **1992**, *13*, 49–54.

(79) Morgan, H.; Green, N. G.; Hughes, M. P.; Monaghan, W.; Tan, T. C. Large-area travelling-wave dielectrophoresis particle separator. *J. Micromech. Microeng.* **1997**, *7*, 65–70.

(80) Ottino, J. M.; Wiggins, S. Introduction: mixing in microfluidics. *Phil. Trans. R. Soc. A* **2004**, *362*, 923–935.

(81) Squires, T. M.; Bazant, M. Z. Breaking symmetries in induced-charge electro-osmosis and electrophoresis. *J. Fluid Mech.* **2006**, *560*, 65–101.

(82) Chang, S. T.; Paunov, V. N.; Petsev, D. N.; Velev, O. D. Remotely powered self-propelling particles and micropumps based on miniature diodes. *Nat. Mater.* **2007**, *6*, 235–240.

(83) Harnett, C. K.; Templeton, J.; Dunphy-Guzman, K. a.; Senousy, Y. M.; Kanouff, M. P. Model based design of a microfluidic mixer driven by induced charge electroosmosis. *Lab Chip* **2008**, *8*, 565–572.

(84) Dittrich, P. S.; Manz, A. Lab-on-a-chip: microfluidics in drug discovery. *Nat. Rev. Drug Discov.* **2006**, *5*, 210–218.

(85) Neuži, P.; Giselbrecht, S.; Länge, K.; Huang, T. J.; Manz, A. Revisiting lab-on-a-chip technology for drug discovery. *Nat. Rev. Drug Discov.* **2012**, *11*, 620–32.

(86) Purcell, E. M. Life at Low Reynolds Number. *Am. J. Phys.* **1977**, *45*, 3–11.

(87) Kowalik, M.; Bishop, K. J. M. Ratcheted electrophoresis of Brownian particles. *Appl. Phys. Lett.* **2016**, *108*, 203103.

(88) Paxton, W. F.; Kistler, K. C.; Olmeda, C. C.; Sen, A.; St Angelo, S. K.; Cao, Y. Y.; Mallouk, T. E.; Lammert, P. E.; Crespi, V. H. Catalytic nanomotors: Autonomous movement of striped nanorods. *J. Am. Chem. Soc.* **2004**, *126*, 13424–13431.

(89) Wang, Y.; Hernandex, R. M.; Bartlett, D. J.; Bingham, J. M.; Kline, T. R.; Sen, A.; Mallouk, T. E. Bipolar electrochemical mechanism for the propulsion of catalytic nanomotors in hydrogen peroxide solutions. *Langmuir* **2006**, *22*, 10451–10456.

(90) Wang, W.; Chiang, T. Y.; Velegol, D.; Mallouk, T. E. Understanding the efficiency of autonomous nano- and microscale motors. *J. Am. Chem. Soc.* **2013**, *135*, 10557–10565.

(91) Bahng, J. H.; Yeom, B.; Wang, Y.; Tung, S. O.; Hoff, J. D.; Kotov, N. Anomalous dispersions of hedgehog' particles. *Nature* **2014**, *517*, 596–599.

(92) Ilievski, F.; Mazzeo, A. D.; Shepherd, R. F.; Chen, X.; Whitesides, G. M. Soft robotics for chemists. *Angew. Chem. Int. Ed.* **2011**, *50*, 1890–1895.

(93) Rus, D.; Tolley, M. T. Design, fabrication and control of soft robots. *Nature* **2015**, *521*, 467–475.

(94) Spellings, M.; Engel, M.; Klotsa, D.; Sabrina, S.; Drews, A. M.; Nguyen, N. H. P.; Bishop, K. J. M.; Glotzer, S. C. Shape control and compartmentalization in active colloidal cells. *Proc. Natl. Acad. Sci. U.S.A.* **2015**, *112*, E4642–50.

TOC Graphic

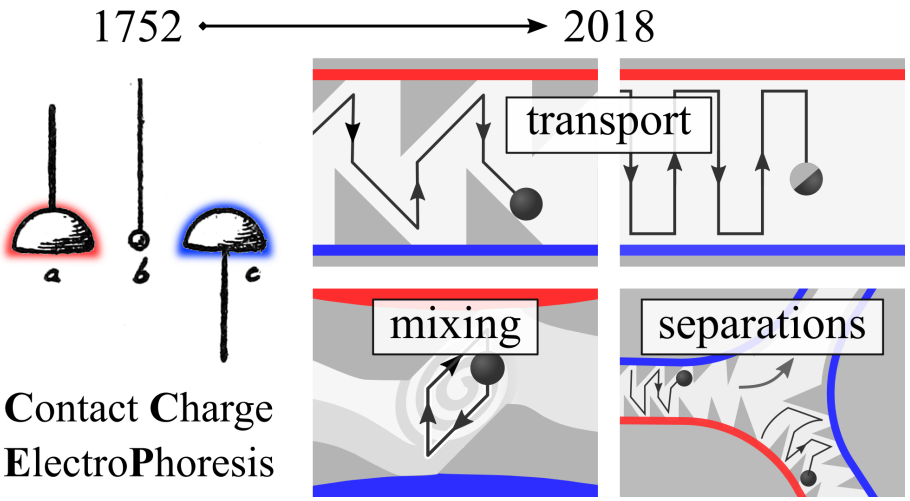
1752
2018
a
b
c
Contact Charge
ElectroPhoresis
transport
mixing
separations

Biographies

Kyle Bishop is an associate professor of chemical engineering at Columbia University. He received his B.S. (2003) from the University of Virginia and his Ph.D. (2009) from Northwestern University, both in chemical engineering. Earlier, he was a post-doctoral scholar in the Department of Chemistry at Harvard University and an assistant professor in the Department of Chemical Engineering at The Pennsylvania State University. His research seeks to discover, understand, and apply new strategies for organizing and directing colloidal matter through self-assembly and self-organization far-from-equilibrium.

Aaron Drews is an assistant teaching professor in chemical engineering at the University of California San Diego. He obtained his Ph.D. (2014) in chemical engineering from The Pennsylvania State University where he helped to develop contact charge electrophoresis in microfluidic devices. He obtained his B.S. (2008) and M.S. (2009) in chemical engineering at The University of Akron. His teaching interests include flipped classrooms, active learning formats, and adding hands-on components to traditional lecture courses.

Charles Cartier is currently a research analyst for CNA, a non-profit consulting company. He graduated with a Ph.D. (2017) in chemical engineering from The Pennsylvania State University and received his B.S. (2012) in chemical engineering from Case Western Reserve University. His research has focused on using electrostatic actuation mechanisms in microscale (colloidal) systems. He is particularly interested in the dynamic collective behaviors that emerge in driven systems comprised of many microscale components.

Shashank Pandey is a graduate student at Columbia University pursuing his Ph.D. degree in chemical engineering in the group of Prof. Kyle Bishop. He received his M.Tech. and B.Tech. (2014) from the Indian Institute of Technology-Kharagpur, India in the Department of Chemical Engineering. His current research interests include the development of simulation tools for modeling contact-charge electrophoresis and the study of pattern formation in arrays of electrostatic oscillators.

Yong Dou is a Ph.D. candidate in the group of Prof. Kyle Bishop in the Department of Chemical Engineering at Columbia University. He received his B.S. (2015) in chemical engineering from Dalian University of Technology. His current research interests include the role of shape and symmetry in directing particle motions via contact charge electrophoresis and the development of soft matter actuators.